Synthesis of and Small Molecule Coordination to Highly Electrophilic Cationic Manganese(I) and Rhenium(I) Carbonyl Complexes with Tied-Back Phosphites

Xinggao Fang, Brian L. Scott, Kevin D. John, and Gregory J. Kubas*

Chemistry Division, MS J514, Los Alamos National Laboratory, Los Alamos, New Mexico 87545

Received June 2, 2000

Formally 16e highly electrophilic fragments $[Mn(CO)_4(L)][BAr_F]$ with a tied-back phosphite ($L = P(OCH_2)_3CMe$) coordinate Et_2O (**5b**) or *cis*-cyclooctene (**5c**) and are prepared by reaction of the neutral methyl complex $Mn(Me)(CO)_4(L)$ with $[H(OEt_2)_2][BAr_F]$ or $[Ph_3C][BAr_F]$ in the presence of *cis*-cyclooctene (cco), respectively. The solvent-bound rhenium complexes $[Re(CO)_4(L)(CH_2Cl_2)][BAr_F]$ (**6a**) and $[Re(CO)_3(L)_2(CH_2Cl_2)][BAr_F]$ (**7a**) are prepared similarly by reaction of the respective neutral precursors with $[Ph_3C][BAr_F]$ in CH_2Cl_2. The CH_2Cl_2 molecule binds tightly to the Re(I) center and could not be removed under high vacuum for hours. However, the CH_2Cl_2 is readily displaced by Et_2O, cco, and Et_3SiH to afford ether-, olefin-, and silane-coordinated complexes **6b**−**d** and **7b**−**d**, respectively. While the η^2-(H−$SiEt_3$)-coordinated **7d** is stable in solution at room temperature and is a rare example of an isolable cationic silane complex, the more electrophilic analogue **6d** readily decomposes at room temperature to give the hydride-bridged complex $\{[cis\text{-}Re(L)(CO)_4]_2(\mu\text{-}H)\}\{BAr_F\}$ (**10**). Solid-state structures of **5c**, **10**, and **7b** have been determined by single-crystal X-ray structural analysis.

Introduction

Studies on the coordination and activation of small molecules such as H_2 and silanes onto electrophilic transition-metal complexes with formally 16e configurations have been an important research theme.[1] The coordination properties of small molecules such as silanes, olefins, and alkanes are clearly determined by the subtle balance of the steric and electronic environments around the metals.[2] In particular, we have been interested in electrophilic Mn(I) complexes such as **1**[3] and **2**,[4] where the counteranion is the weakly coordinating BAr_F (Chart 1).[5] In these complexes and their Re(I) analogues,[2b] the phosphine ligand exhibits agostic C−H interactions to the metals that can be displaced by the H_2 ligand. However, other weak ligands such as the solvent molecules CH_2Cl_2 and Et_2O do not bind, possibly because of the bulky environment around the metals. Albertin et al. recently reported the analogous anion-coordinated phosphite complex **3** and its Re(I) analogue.[6] Apparently the anion $CF_3SO_3^-$ binds to the in situ generated Mn(I) cation, preventing coordination of neutral solvent molecules. It is reasonable to assume that the phosphite would exhibit agostic binding to Mn(I) if a noncoordinating anion such as BAr_F were used. A series of tetracarbonyl complexes of the type $[cis\text{-}Mn(CO)_4(P)(L')][BF_4]$ with stronger σ donors L′ such as H_2O, R_2S, and NCMe ($P = PR_3$, $PPh(OMe)_2$) has also been reported.[7] Here the L′ ligands bind to this electrophilic metal cation rather than the BF_4, which is a known coordinating anion.

We felt it was of interest to study metal complexes based on tied-back phosphites incapable of forming agostic interactions, thus eliminating competition from entropically favored intramolecular C−H interactions for binding of external ligands. This could be very important for the coordination of weak external ligands such as alkanes. A ^{31}P NMR handle would still be retained, along with the steric stabilization provided by large ligands. Phosphites are also much less basic than phosphines and are moderate π-acceptors, thus allowing

* To whom correspondence should be addressed. E-mail: kubas@lanl.gov.

(1) (a) Jessop, P. G.; Morris, R. H. *Coord. Chem. Rev.* **1992**, *121*, 289. (b) Crabtree, R. H. *Angew. Chem., Int. Ed. Engl.* **1992**, *32*, 789. (c) Heinekey, D. M.; Oldham, J. W., Jr. *Chem. Rev.* **1993**, *93*, 913. (d) Schneider, J. J. *Angew. Chem., Int. Ed. Engl.* **1996**, *35*, 1068. (e) Corey, J. Y.; Braddock-Wilking, J. *Chem. Rev.* **1999**, *99*, 175.

(2) For selected recent examples, see: (a) Vigalok, A.; Ben-David, Y.; Milstein, D. *Organometallics* **1996**, *15*, 1839. (b) Heinekey, D. M.; Radzewich, C. E.; Voges, M. H.; Schomber, B. M. *J. Am. Chem. Soc.* **1997**, *119*, 4172. (c) Schlaf, M.; Lough, A. J.; Morris, R. H. *Organometallics* **1997**, *16*, 1253. (d) Martelletti, A.; Gramlich, V.; Zurcher, F.; Mezzetti, A. *New J. Chem.* **1999**, 199. (e) Barthazy, P.; Worle, M.; Mezzetti, A. *J. Am. Chem. Soc.* **1999**, *121*, 480. (f) Albertin, G.; Antoniutti, S.; Bordignon, E.; Carlon, M. *Organometallics* **1999**, *18*, 2052. (g) Becker, T. M.; Krause-Bauer, J. A.; Homrighausen, C. L.; Orchin, M. *Polyhedron* **1999**, *18*, 2563. (h) Butts, M. D.; Kubas, G. J.; Luo, X.-L.; Bryan, J. C. *Inorg. Chem.* **1997**, *36*, 3341. (i) Huhmann-Vincent, J.; Scott, B. L.; Kubas, G. J. *J. Am. Chem. Soc.* **1998**, *120*, 6808. (j) Huhmann-Vincent, J.; Scott, B. L.; Kubas, G. J. *Inorg. Chem.* **1999**, *38*, 115. (k) Huhmann-Vincent, J.; Scott, B. L.; Kubas, G. J. *Inorg. Chim. Acta.* **1999**, *294*, 240.

(3) (a) King, W. A.; Luo, X.-L.; Scott, B. L.; Kubas, G. J.; Zilm, D. W. *J. Am. Chem. Soc.* **1996**, *118*, 6782. (b) King, W. A.; Scott, B. L.; Eckert, J.; Kubas, G. J. *Inorg. Chem.* **1999**, *38*, 1069.

(4) Toupadakis, A.; Kubas, G. J.; King, W. A.; Scott, B. L.; Huhmann-Vincent, J. *Organometallics* **1998**, *17*, 5315.

(5) Brookhart, M.; Grant, B.; Volpe, A. F., Jr. *Organometallics* **1992**, *11*, 3920.

(6) (a) Albertin, G.; Antoniutti, S.; Bettiol, M.; Bordignon, E.; Busatto, F. *Organometallics* **1997**, *16*, 4959. (b) Albertin, G.; Antoniutti, S.; Garcia-Fontan, S.; Carballo, R.; Padoan, F. *J. Chem. Soc., Dalton Trans.* **1998**, 2071.

(7) Harris, P. J.; Knox, S. A. R.; McKinney, R. J.; Stone, F. G. A. *J. Chem. Soc., Dalton Trans.* **1978**, 1009.

10.1021/om0004693 CCC: $19.00
Publication on Web 09/01/2000

Chart 1

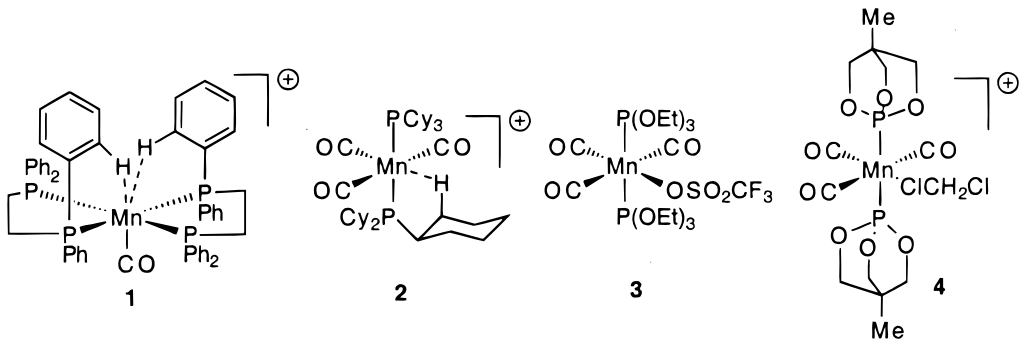

the design of highly Lewis acidic centers ("superelectrophiles") to attract the electron density of C−H bonds. The cationic metal center (with low-interacting anion) thus could mimic the H^+ of a superacid (with similarly low-interacting anion), and metallocarbocation-like species, e.g. $[L_nMCH_4]^+$, could be isolable. Such transient species have been implicated in the nonradical mechanisms of oxidase enzymes such as certain methane monooxygenases (MMO), where M is high-valent Fe(IV).[8] Furthermore, in $L_nM(CH_4)^+$ the alkane proton should become very acidic and the extremely mobile H^+ can transfer very rapidly to a nearby cis-ligand or an external base:

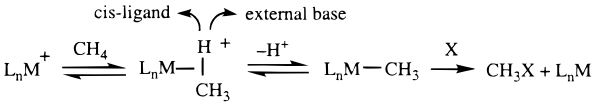

Such *heterolytic cleavage* of a σ-bonded molecule (H_2, hydrocarbons, etc.) is undoubtedly the key step in many catalyses, including biocatalytic splitting of H_2 in hydrogenases,[2k] yet it has not been extensively studied except for intramolecular proton exchange processes in $MH(\eta^2\text{-}H_2)$ systems.

We have synthesized the Mn(I) precursor complex **4** with three CO and two tied-back phosphites, $P(OCH_2)_3CMe$ (L), as ligands and an easily displaceable solvent molecule, CH_2Cl_2, as the sixth ligand.[9] The phosphite L originally prepared by Verkade[10] is not only a weaker σ donor and stronger π acceptor than respective phosphines but is also more compact, thus affording a more electrophilic M(I) cationic center with more open space for the coordination of silanes, olefins, or other sixth ligands, possibly alkanes.[9] Here we wish to report on the synthesis and small molecule binding properties of the related five-coordinate fragments **5**−**7** using the same phosphite L on Re as well as Mn (Chart 2). **5**−**7** bind either a solvent molecule or small molecules such as silanes and olefins, and the counteranion is noncoordinating BAr_F. There are significant differences in the stability and stereochemistry of the first-row versus third-row metal systems, e.g. the cis-phosphite configuration in **7** versus trans in **4**. The latter relates to the smaller size of Mn, which would lead to increased steric repulsions between cis phosphites, which are favored electronically (Chart 2).

Chart 2

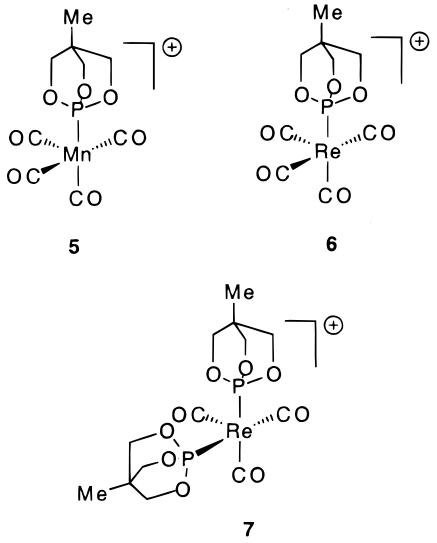

Scheme 1

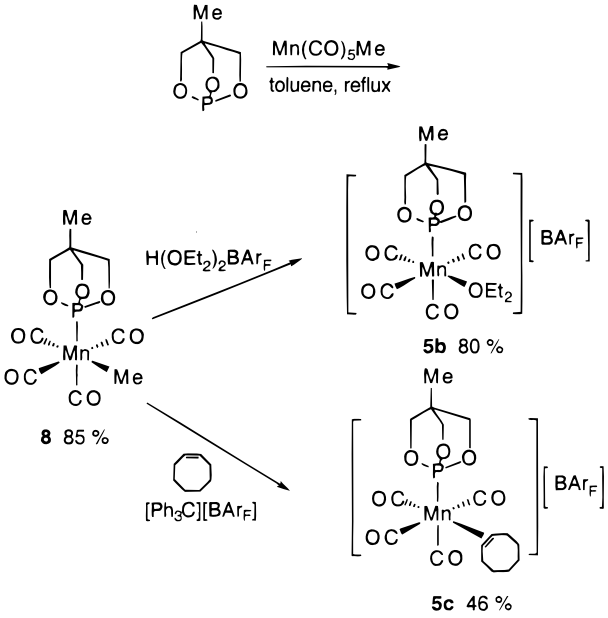

Results and Discussion

[*cis*-Mn(L)(CO)$_4$(solvent)][BAr$_F$] (5). Derivatives of complex **5** are prepared in the same manner as that for

(8) (a) Feig, A. L.; Lippard, S. J. *Chem. Rev.* **1994**, *94*, 759. (b) Valentine, A. M.; Stahl, S. S.; Lippard, S. J. *J. Am. Chem. Soc.* **1999**, *121*, 3876. (c) Choi, S.-Y.; Eaton, P. E.; Kopp, D. A.; Lippard, S. J.; Newcomb, M.; Shen, R. *J. Am. Chem. Soc.* **1999**, *121*, 12198.

(9) Fang, X.-G.; Huhmann-Vincent, J.; Scott, B. L.; Kubas, G. J. *J. Organomet. Chem.*, in press.

(10) Verkade, J. G.; Huttemann, T. J.; Fung, M. K. *Inorg. Chem.* **1965**, *4*, 83.

Table 1. IR and ^{31}P NMR Spectral Data for Complexes 4−11

complex	IR (CD_2Cl_2; ν_{CO}, cm^{-1})	^{31}P (CD_2Cl_2, room temp; δ)
4[a]	2096 w, 2025 vs, 2004 s	155.2
5b	2123 m, 2039 s, 2011 s	149.0
5c	2115 m, 2057 s, 2040 s	151.2
6a	2139 m, 2049 vs, 2019 s	103.9
6b	2131 m, 2033 vs, 2001 s	107.1
6c	2130 m, 2056 s, 2042 vs, 2027 s	98.6
7a	2088 s, 2025 s, 1991 s	108.1
7b	2078 s, 2009 s, 1971 s	111.4
7c	2081 s, 2018 s, 2003 s	102.3
7d	2080 s, 2044 s, 2015 s, 1751 m[b]	106.6
8	2073 m, 1982 s, 1952 s	162.5[c]
9	2090 m, 1986 vs, 1944 s	99.8[c]
10	2132 w, 2115 s, 2047 vs, 2025 s, 2009 s	97.8
11	2035 s, 1964 s, 1915 s	102.4

[a] CH_2Cl_2 coordinated.[9] [b] Re−H−Si stretch. [c] Solvent is $CDCl_3$.

the synthesis of **4** as shown in Scheme 1. Reaction of $Mn(CO)_5Me$[11] with 1 equiv of L[10] in refluxing toluene affords the known neutral methyl precursor **8**.[12] Unfortunately, attempted extraction of the methyl group by reaction of **8** with $[Ph_3C][BAr_F]$[13] in CH_2Cl_2 gives only a mixture of products from which no single compound could be isolated. It is possible that the expected CH_2Cl_2 complex **5a** is not as stable as the analogous CH_2Cl_2-bound **4a**, containing two phosphite groups, because of its more electrophilic nature. However, if the reaction is carried out in the presence of *cis*-cyclooctene (cco) at low temperature, the olefin-bound complex **5c** could be isolated as yellow crystals in 46% yield. In addition, the methyl group in **8** could be protonated off with $H(OEt_2)_2BAr_F$ to afford the ether-bound complex **5b** as colorless crystals (Scheme 1). The Et_2O and cco molecules in **5b**,**c** are tightly bound to the Mn(I) center and cannot be removed under high vacuum for hours. The bound Et_2O has a ^{1}H NMR signal at 3.52 ppm (OCH_2) and a ^{13}C NMR signal at 77.0 ppm (OCH_2), both shifted downfield relative to the free ether (δ 3.27 (OCH_2), 65.6 (OCH_2)). This is clearly consistent with the transfer of electron density from the oxygen atom of the ether to the highly electrophilic Mn(I). The bound cco molecule has NMR signals for the olefinic group (δ 4.94 (C*H*) and 101.8 (*C*H)) shifted upfield from those of the free cco (δ 5.69 (C*H*) and 130.2 (*C*H)), which is quite typical for olefin bound to a transition metal. The CO stretching frequencies for **5b,c** (Table 1) are consistent with electrophilic metal centers (see below) and are comparable to those for $[Mn(CO)_4(H_2O)\{PPh(OMe)_2\}][BF_4]$.[7] $P(OR)_3$ derivatives of the latter could not be isolated, however.

Solid-state structures of **5b**,**c** have been obtained from single-crystal X-ray structural analysis. While the structure of **5b** is highly disordered, the structure of **5c** is well-determined (Figure 1). The crystallographic data are listed in Table 2. The complex **5c** shows an octahedral structure around Mn(I). The Mn−C(1) and Mn−C(2) distances are 2.3966(40) and 2.4032(41) Å, respectively. These distances are significantly longer than those of 2.233 and 2.229 Å found in $[Mn_2(\mu\text{-}PPh_2CH{=}CH_2)(CO)_7(PEt_3)]$, one of the closest structurally characterized Mn−olefin analogues in the Cambridge Crystal Structure Database.[14] More interestingly, the olefinic C(1)−C(2) distance of 1.3582(54) Å is very close to the distance of a free double bond at 1.34 Å. This indicates there is very little π back-donation from Mn(I) to the coordinated double bond. Accordingly, the Mn−C(11) distance trans to the bound cco, 1.8277(53) Å, is shorter than all other Mn−C distances of Mn−C(9), Mn−C(10), and Mn−C(12) at 1.8578(51), 1.8585(52), and 1.8577-

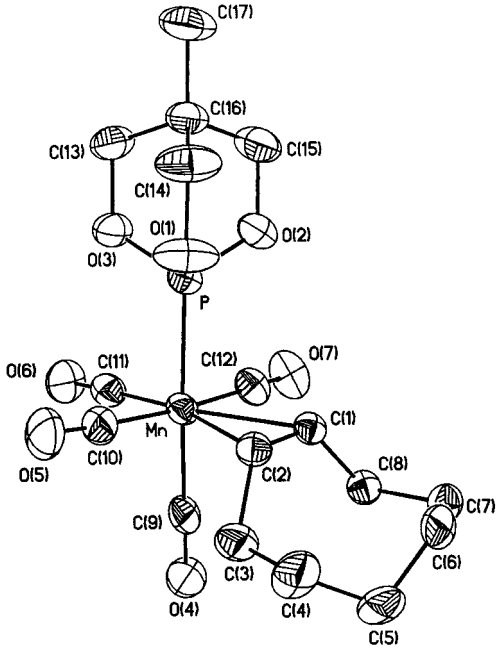

Figure 1. Drawing of [*cis*-Mn(L)$(CO)_4$(*cis*-cyclooctene)]-$[BAr_F]$ (**5c**) (thermal ellipsoids are drawn at the 35% level). Selected bond distances (Å) and angles (deg): Mn−C(1), 2.3966(40); Mn−C(2), 2.4032(41); C(1)−C(2), 1.3582(54); Mn−P, 2.2510(12); Mn−C(11), 1.8277(53); Mn−C(9), 1.8578-(51); Mn−C(10), 1.8585(52); Mn−C(12), 1.8577(52); C(9)−Mn−P, 177.80(0.15); C(10)−Mn−C(12), 173.91(0.21).

Table 2. Crystallographic Data for Compounds 5c, 10, and 7b[a]

	5c[b]	**10**[c]	**7b**[d]
empirical formula	$C_{49}H_{27}BF_{24}MnO_7P$	$C_{50}H_{31}BF_{24}O_{14}P_2Re_2$	$C_{49}H_{40}BF_{24}O_{10}P_2Re$
fw	1280.43	1756.90	1503.76
space group	$P2_1/n$	$C2/c$	$P\bar{1}$
λ (Å)	0.710 73	0.710 73	0.710 73
temp (K)	230(2)	203(2)	203(2)
a (Å)	18.1505(9)	19.707(1)	12.9841(9)
b (Å)	14.6079(7)	16.5848(8)	14.202(1)
c (Å)	21.074(1)	18.538(1)	16.321(1)
α (deg)	90	90	91.325(1)
β (deg)	101.339(1)	94.600(1)	98.447(1)
γ (deg)	90	90	102.836(2)
V (Å^3)	5478.6(5)	6039.5(5)	2897.8(4)
Z	4	4	2
ρ_{calcd} (g cm^{-3})	1.552	1.932	1.732
μ (cm^{-1})	0.0400	0.4193	0.2283
final R indices			
R1	0.0602	0.0277	0.0644
wR2	0.1761	0.0811	0.1152

[a] $R1 = \sum||F_o| - |F_c||/\sum|F_o|$ and $wR2 = [\sum[w(F_o^2 - F_c^2)^2]/\sum[w(F_o^2)^2]]^{1/2}$. [b] The parameter $w = 1/[\sigma^2(F_o^2) + (0.1289P)^2]$. [c] The parameter $w = 1/[\sigma^2(F_o^2) + (0.0458P)^2$. [d] The parameter $w = 1/[\sigma^2(F_o^2) + (0.0372P)^2]$.

(11) Closson, R. D.; Kozikowski, J.; Coffield, T. H. *J. Org. Chem.* **1957**, *22*, 598.
(12) Green, M.; Hancock, R. I.; Wood, D. C. *J. Chem. Soc. A* **1968**, 2718.
(13) Bahr, S. R.; Boudjouk, P. *J. Org. Chem.* **1992**, *57*, 5545.
(14) Henrick, K.; McPartlin, M.; Iggo, J. A.; Kemball, A. C.; Mays, M. J.; Raithby, P. R. *J. Chem. Soc., Dalton Trans.* **1987**, 2669.

Scheme 2

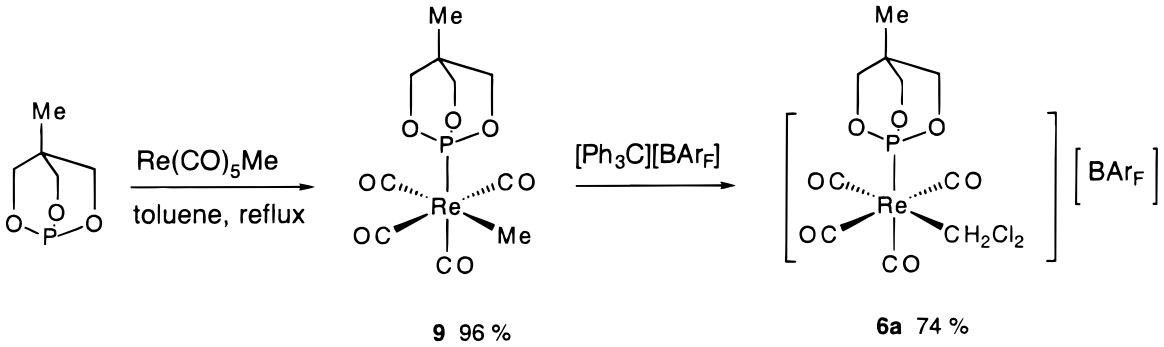

Scheme 3

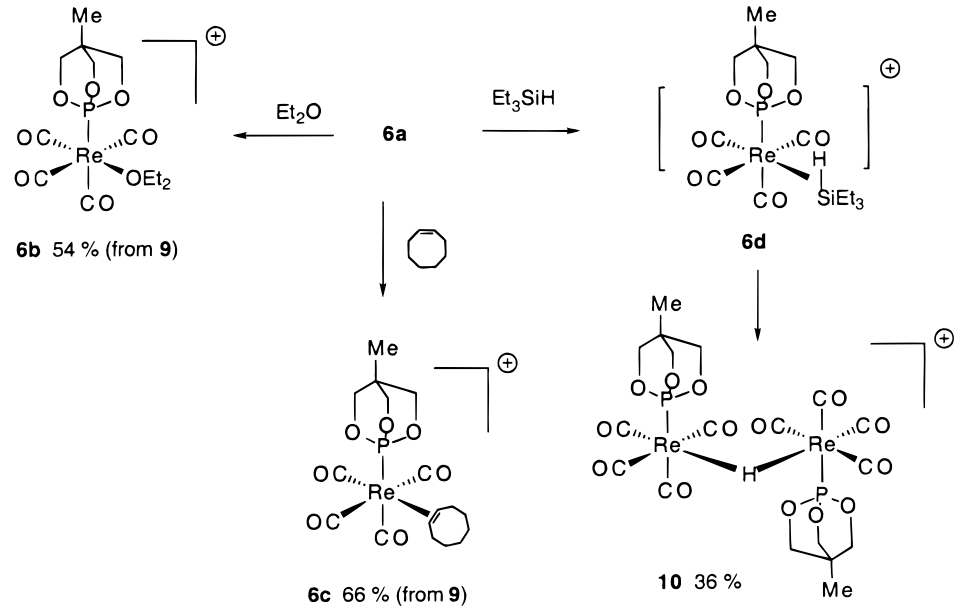

(52) Å, respectively. The C(9)−Mn−P angle of 177.80-(0.15)° is almost linear, while the C(10)−Mn−C(12) angle of 173.91(0.21)° slightly deviates from linearity, bent away from the bound cco. Another interesting feature of the structure **5c** is that the olefin double bond is perpendicular to the P−Mn−C(9) axis, even though a parallel orientation was usually observed in similar complexes for effective π-bonding between the two fragments, e.g. $ReH_3(PMe_2Ph)_3(\eta^2\text{-}C_5H_8)$[15a] and $ReH_3(C_2H_4)_2(P^iPr_2Ph)_2$.[15b] Apparently the parallel orientation here would generate an unfavorable steric interaction of the olefin with the phosphite. Electronically the phosphite is not a strong donor like a phosphine but is more like a CO; therefore, there is probably not a strong electronic preference and even a small steric effect can dictate the olefin orientation (Table 2 and Figure 1).

[*cis*-Re(L)(CO)$_4$(solvent)][BAr$_F$] (6). We hypothesize that the unsuccessful isolation of **5a** is due to the highly electrophilic nature of the Mn(I) complex, which might cause cleavage of bound CH_2Cl_2. A Re(I) complex bound to CH_2Cl_2 should be more electron-rich and might be more stable, similar to the analogous phosphine complex $[Re(CO)_4(PR_3)(CH_2Cl_2)]^+$, which can be isolated but is subject to nucleophilic attack by OEt_2 to give $\{[Re(CO)_4(PR_3)]_2(\mu\text{-Cl})\}^+$.[2j] We have thus similarly synthesized the solvent CH_2Cl_2 bound Re(I) complex **6a** (Scheme 2), which is indeed more stable and is isolated as brick-shaped light yellow crystals.

In analogy to **4**, the CH_2Cl_2 molecule binds tightly to the Re(I) center in **6a** and could not be removed under high vacuum for hours. While **6a** is not as electrophilic as the unseen Mn(I) congener, it appears to be more electrophilic than the Mn(I) complex **4** with two phosphites. This is evidenced by the higher ν_{CO} (cm^{-1}) values of **6a** at 2139 m, 2049 vs, and 2019 s in comparison to those of **4** at 2096 w, 2025 vs, and 2004 s (Table 1). Unfortunately, the X-ray structure of **6a** could not be determined because it is highly disordered.

The bound CH_2Cl_2 in **6a** can readily be displaced by ether, cco, and silanes to give **6b**−**d**, respectively (Scheme 3). As observed for the analogous adducts of **5**, the NMR signals of bound Et_2O, δ 3.99 (OCH_2) and 80.2 (OCH_2), shift downfield relative to those of free Et_2O; the signals corresponding to the olefinic group of bound cco at δ 5.15 (C*H*) and 97.6 (*C*H) shift upfield in relation to free cco.

The ^{1}H NMR spectrum of the η^2-H−SiEt$_3$ ligand in **6d** shows a broad peak at −10.68 ppm, corresponding to the Si−*H* proton. This new signal is similar to those for the silane σ ligands in **4**−$SiHEt_3$[9] and $[Re(CO)_4(PR_3)(SiHEt_3)]^+$ [2k] detected at low temperature. Similar to **4**−$SiHEt_3$, **6d** is thermally unstable. Unlike **4**−$SiHEt_3$, which did not yield an isolable complex after decomposition, **6d** decomposes at room temperature within 10 min to give the hydride-bridged dimer **10**, which is isolated as stable colorless crystals in 36% yield via crystalliza-

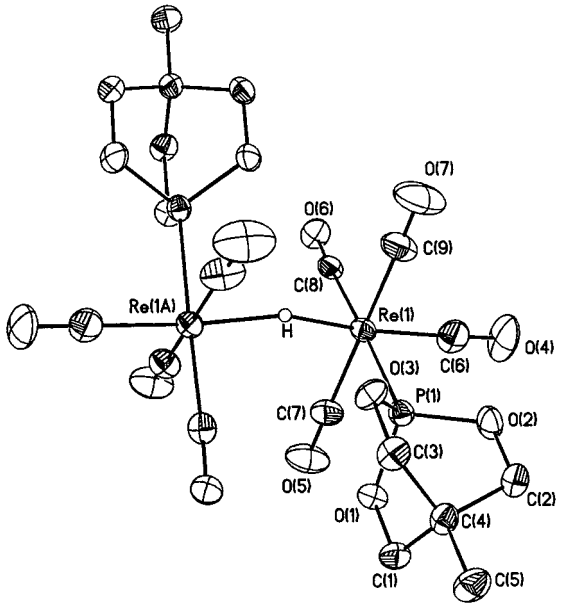

Figure 2. Drawing of {[*cis*-Re(L)$(CO)_4]_2(\mu$-H)}{BAr_F} (**10**) (thermal ellipsoids are drawn at the 35% level). Selected bond distances (Å) and angles (deg): Re(1)−H, 1.7617(185); Re(1)−C(6), 1.9406(64); Re(1)−C(7), 1.9919(65); Re(1)−C(8), 1.9880(52); Re(1)−P(1), 2.3735(12); Re(1)−H−Re(1A), 156.5; Re(1)−C(6)−H, 171.64(2.90); H−Re(1)−C(7), 96.09(2.78); H−Re(1)−C(8), 92.30(0.74); H−Re(1)−C(9), 80.59(2.84); H−Re(1)−P(1), 85.85.

tion from CH_2Cl_2/hexane. Heterolytic cleavage of the Si−H bond presumably occurs as for the phosphine system. The ^{1}H NMR spectrum of **10** displays a triplet at δ −18.23 for the μ-H ligand, with a J_{PH} value of 12.2 Hz, comparable to the signals for the phosphine analogues $\{[Re(CO)_4(PR_3)]_2(\mu\text{-H})\}^+$: δ −17.59 (J_{PH} = 7.8) for R = Cy and δ −15.56 (J_{PH} = 10.0) for R = Ph.[2k] GC-MS analysis of the volatiles of the reaction mixture shows Et_3SiCl and $(Et_3Si)_2O$ as major components, indicating solvent CH_2Cl_2 might attack the highly activated silicon atom of the bound silane to cause H−Si cleavage. $(Et_3Si)_2O$ is presumably generated from the reaction of Et_3SiCl and/or Et_3Si^+ with adventitious moisture as for **4**−$SiHEt_3$,[9] $[Re(CO)_4(PR_3)(SiHEt_3)]^+$,[2k] and $[CpFe(CO)(PPh_3)(SiHR_3)]^+$.[16]

Single crystals of **10** suitable for X-ray structural analysis are grown from the solvent mixture CH_2Cl_2/hexane at −30 °C, and the solid-state structure is solved by single-crystal structural analysis (Figure 2). The crystallographic data are listed in Table 2. The structure shows the hydrogen atom on the 2-fold rotation axis of the two Re(I) fragments, where each fragment is octahedral around the Re(I) center. This orientation is in contrast with that of the PPh_3 analogue {[*cis*-Re(PPh_3)-$(CO)_4]_2(\mu$-H)}{BAr_F},[2k] where the two Re(I) fragments are located on the same side. The position of the hydride is refined, and the average Re−H distance is 1.7617-(185) Å, which is considerably shorter than the 1.91 Å found in the above phosphine analogue. The shorter Re−H distance demonstrates stronger Re−H bonding, which is consistent with a more electron deficient Re(I) cationic center due to the weaker electron donating ability of phosphite in relation to PPh_3. In addition, the Re1−H−Re1A angle of 156.5° is also significantly larger than the 124.4° found in the above phosphine analogue. This structural feature is consistent with a two-electron, three-atom bonding mode around Re1−H−Re1A (Figure 2).

[*fac*-Re$(L)_2(CO)_3$(solvent)][BAr_F] (7). Two tied-back phosphite coordinated Re(I) complexes, analogues of **4**, have also been synthesized, as shown in Scheme 4. The Et_2O-bound **7b** is prepared by reacting the neutral precursor **11** with $H(OEt_2)_2BAr_F$ in 82% yield. **7b** could also be prepared by reaction of **7a** with Et_2O. Interestingly, the phosphites in **7** adopt a cis orientation to each other instead of the trans orientation as found for the $P(OEt)_3$ analogue $\{ReH(CO)_3[P(OEt_3)_2]\}$[7] and the Mn(I) analogue **4**. The cis orientation is evidenced by its CO IR stretching pattern. For instance, ν_{CO} (cm^{-1}) of **7a** shows three strong adsorption peaks at 2088 s, 2025 s, and 1991 s, which is a typical pattern for this type of configuration. This cis orientation is likely determined by a favorable electronic factor without significant steric interference. On the other hand, for the Mn(I) complex **4**, a cis orientation would cause a repulsive interaction between the two phosphites because of the smaller size of Mn(I) in relation to Re(I).

Complex fragment **7** is the least electrophilic among all four cationic fragments **4**−**7** in this study, as can be seen by the IR data in Table 1. However, it still binds the solvent molecule CH_2Cl_2 very tightly. The bound CH_2Cl_2 cannot be removed under high vacuum for hours. As usual, the CH_2Cl_2 can be readily displaced by Et_2O, cco, and Et_3SiH to afford **7b**−**d**, respectively (Scheme 5). In contrast to the previously observed heterolytic H−Si bond cleavage in **6d**, the σ-coordinated silane in **7d** is stable both in the solid state and in solution, similar to the structurally characterized neutral complex $Mo(CO)(\eta^2\text{-H}-SiH_2Ph)(Et_2PC_2H_4PEt_2)_2$.[17] An IR band for the Re−H−Si stretch in **7d** is observed at 1751 cm^{-1}, comparable to that for the Mo complex (1742 cm^{-1}). The solution ^{1}H NMR spectrum of **7d** suggests that the Si−H binds strongly to the cationic Re(I) center. The Si−*H* signal shows a triplet at δ −10.43 with J_{PH} = 12.7 Hz. The signal is blanketed by a Si−H sideband with a J_{SiH} value of 66 Hz, much smaller than the 177 Hz value found in free Et_3SiH, clearly indicating that the Si−H bond is highly stretched.[1e] The solid-state structure of **7d** could not be obtained, because the X-ray structure is highly disordered.

The cis orientation of the two phosphites in **7** is confirmed by an X-ray single-crystal structure analysis of **7b** (Figure 3). The crystallographic data are listed in Table 2. The structure adopts an overall octahedral configuration around Re(I). The Re−O(10) distance is 2.331(81) Å, which is slightly longer than the distance of 2.254(11) Å found in $[Re(CO)_4(PPh_3)(OEt_2)][BAr_F]$.[2i] The respective Re−P(1) and Re−P(2) distances, 2.3746-(29) and 2.3816(29) Å, are similar to those found in **10**. The average Re−C distance trans to the phosphite is 1.9824(130) Å, which is longer than the Re−C distance

(15) (a) Green, M. A.; Huffman, J. C.; Caulton, K. G.; Rybak, W. K.; Ziolkowski, J. J. *J. Organomet. Chem.* **1981**, *218*, C39. (b) Hazel, N. J.; Howard, J. A. K.; Spencer, J. L. *J. Chem. Soc., Chem. Commun.* **1984**, 1663.

(16) (a) Scharrer, E.; Chang, S.; Brookhart, M. *Organometallics* **1995**, *14*, 5686. (b) Chang, S.; Scharrer, E.; Brookhart, M. *J. Mol. Catal. A* **1998**, *130*, 107.

(17) Luo, X.-L.; Kubas, G. J.; Bryan, J. C.; Burns, C. J.; Unkefer, C. J. *J. Am. Chem. Soc.* **1994**, *116*, 10312.

Scheme 4

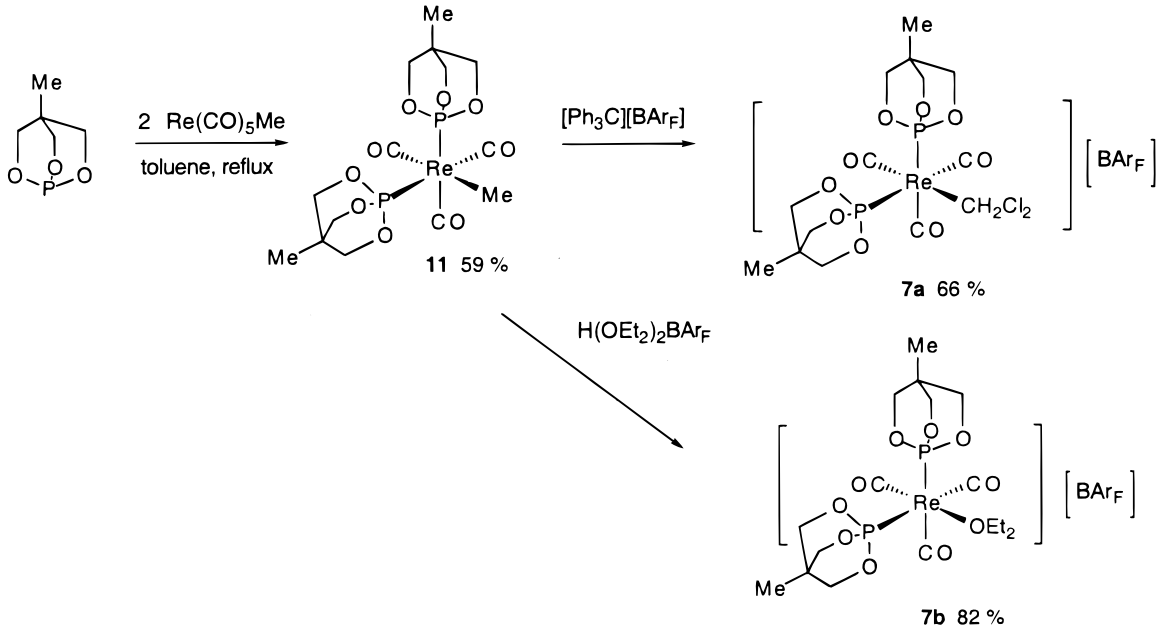

Scheme 5

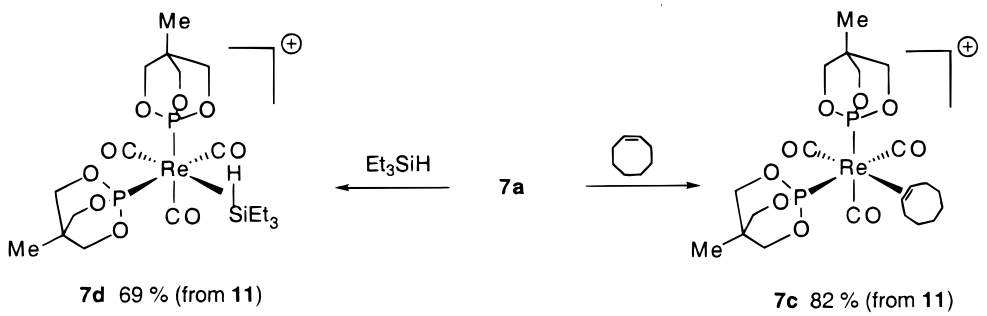

opposite to the bound ether, 1.8579(142) Å. The P(1)−Re(1)−P(2) angle is 93.27(10)°, slightly larger than 90°. The average of the P(1)−Re(1)−C(13) and P(2)−Re(1)−C(11) angles is 87.94(33)°. The C(14)−O(10)−C(16) angle, 111.12(1.04)°, is typical of other M−Et_2O structures.[18]

Comparison of Phosphite to Phosphine Complexes and Summary. The tied-back phosphite complexes are clearly more electrophilic than corresponding phosphine complexes, including triphenylphosphine systems. Table 3compares IR data, and in all cases the ν_{CO} values are higher for the phosphite systems, consistent with a more electron-poor metal center (lower M→CO back-donation). This extends to the hydride-bridged dinuclear phosphite complex **10**, which has a slightly higher ν_{CO} value (10−20 cm^{-1}) than {[*cis*-Re(PR$_3$)(CO)$_4$]$_2$(μ-H)}{BAr$_F$}.[2k] The cationic Re complexes have higher frequencies than the neutral Re−Me complexes. The Mn complexes have slightly higher ν_{CO} values than the Re analogues because first-row metals are less electron rich than third-row metals. Thus, the [Mn(L)(CO)$_4$(L′)][BAr$_F$] species **5b** (L′ = Et_2O) and **5c** (L′ = cco) have the most electrophilic metal centers. The CO stretching frequencies (Table 1) increase in the order **4** < **5b** < **5c**, indicating that the electrophilicity of the Mn(I) center increases in the same order, **4** < **5b** < **5c**. The third-row complexes with two phosphites, [Re(L)$_2$(CO)$_3$(L′)][BAr$_F$] (**7**), have the least electrophilic centers. Thus, while **7d** (L′ = η^2-H−$SiEt_3$) is stable in solution at room temperature, the more electrophilic analogue **6d** readily heterolytically cleaves the bound silane at room temperature to give net elimination of $SiEt_3^+$ and formation of **10**. The Si center is more electropositive (δ+) in the tetracarbonyl **6d** than in the tricarbonyl **7d**. It is somewhat surprising that **7d** is stable, since isolable cationic silane complexes are very rare because the Si atom of the Si−H bond is highly activated toward nucleophilic attack.

None of these cationic fragments bind N_2, as was also the case for the phosphine fragments [Re(CO)$_4$(PR$_3$)][BAr$_F$] and [Mn(CO)$_3$(PR$_3$)$_2$][BAr$_F$]. As previously discussed, there is not enough back-donation from the metal to N_2 to stabilize binding (N_2 is a very poor σ donor, weaker than even CH_2Cl_2, and relies on good back-donation to bind to metal centers).[4] H_2 and σ H−X bonded ligands in general bind more strongly relative to N_2 as the electrophilicity of the metal center increases. This is important in biological systems such as hydrogenase enzymes, where H_2 preferentially binds to and is activated on iron centers that, significantly,

(18) (a) Yi, C. S.; Wodka, D.; Rheingold, A. L.; Yap, G. P. A. *Organometallics* **1996**, *15*, 2. (b) Rix, F. C.; Brookhart, M.; White, P. S. *J. Am. Chem. Soc.* **1996**, *118*, 2436. (c) Solari, E.; Musso, F.; Gallo, E.; Gloriani, C. R. N.; Chiesi-Villa, A.; Rizzoli, C. *Organometallics* **1995**, *14*, 2265.

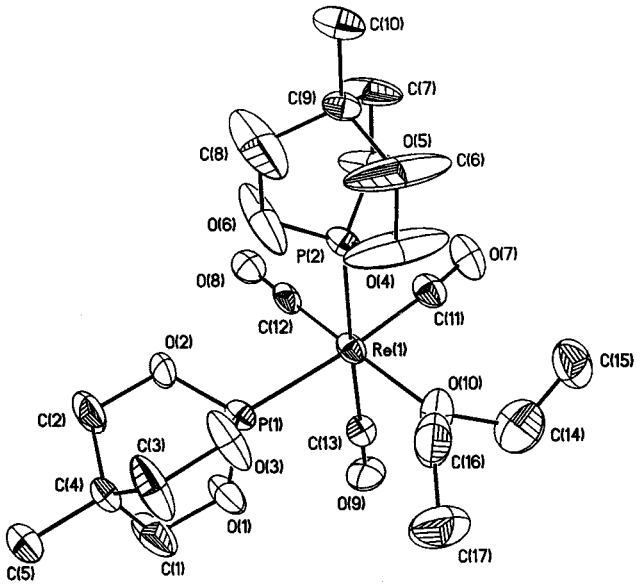

Figure 3. Drawing of [*fac*-Re(L)$_2$(CO)$_3$(OEt$_2$)][BAr$_F$] (**7b**) (thermal ellipsoids are drawn at the 35% level). Selected bond distances (Å) and angles (deg): Re(1)−O(10), 2.2331(81); Re(1)−P(1), 2.3746(29); Re(1)−P(2), 2.3816(29); Re(1)−C(11), 1.9640(133); Re(1)−C(12), 1.8579(142); O(10)−C(14), 1.5720(172); O(10)−C(16), 1.4565(177); O(10)−Re(1)−C(12), 178.40(0.42); C(13)−Re(1)−P(2), 177.40(0.34); P(2)−Re(1)−P(1), 93.27(0.10); P(2)−Re(1)−C(11), 87.79(0.34); C(14)−O(10)−C(16), 111.12(1.04).

Table 3. Comparison of ν_{CO} Values for Tied-Back Phosphite (L) and Phosphine Complexes

complex	ν_{CO}, cm^{-1}
[Mn(L)(CO)$_4$(Et$_2$O)]$^+$	2123 m, 2039 s, 2011 s
[Re(L)(CO)$_4$(Et$_2$O)]$^+$	2131 m, 2033 vs, 2001 s
[Re(PPh$_3$)(CO)$_4$(Et$_2$O)]$^+$	2118 m, 2010 vs, 1988 s
[Re(PCy$_3$)(CO)$_4$(Et$_2$O)]$^+$	2111 m, 1999 vs, 1974 s
Re(Me)(L)(CO)$_4$	2090 m, 1986 vs, 1944 s
Re(Me)(PPh$_3$)(CO)$_4$	2077 m, 1973 vs, 1935 s
Re(Me)(PCy$_3$)(CO)$_4$	2070 m, 1969 vs, 1924 s

contain CO ligands to increase the electrophilicity of Fe and also facilitate reversible binding of H_2.[2k] Because of their strong trans influence, CO ligands almost invariably weaken the binding of σ ligands such as H_2 trans to them because H_2 and X−H ligands are good π acceptors that also need back-donation (though not as much as N_2). Conversely, the binding of normally weak pure σ donors such as Et_2O and CH_2Cl_2 are greatly enhanced on electrophilic centers with CO trans to them. The coordination to the fragments **5**−**7** and also [Re(PR$_3$)(CO)$_4$]$^+$ is irreversible, although the more electron rich species [Mn(PR$_3$)$_2$(CO)$_3$]$^+$ (**2**) and also **1** do not bind these ligands. However, the latter have competing internal agostic C−H interactions that are entropically favored over weak external ligand binding; therefore, it is difficult to sort out the effects here. Thus, the tied-back phosphite ligands that cannot give agostic interactions are clearly advantageous for studying extremely weak ligand coordination.

In summary, the highly electrophilic cationic Mn(I) and Re(I) complexes **5**−**7** with tied-back phosphite ligands and a noncoordinating BAr$_F$ anion have been synthesized. These complexes are more electrophilic and sterically less congested than the analogous phosphine complexes, which favors strong binding of weak solvento ligands, e.g. CH_2Cl_2 and Et_2O, and also *cis*-cycloolefin. While binding of Et_3SiH to **7a** affords stable Si−H σ-coordinated **7d**, binding to the more electrophilic **6a** leads to thermally unstable **6d** from which the hydride-bridged dimer **10** forms via heterolytic Si−H cleavage. It should be noted that in order to observe binding of extremely weak ligands such as alkanes to these highly electrophilic 16e metal centers, a ligand system must be designed such that the resulting complexes are soluble in hydrocarbons rather than polar solvents. Another approach would be to sterically protect the metal with bulky ligands to inhibit coordination of bulky polar molecules that could be used as the solvent for cationic complexes. Work in these directions is in progress in our laboratory.

Experimental Section

All manipulations were performed either under a helium atmosphere in a Vacuum Atmospheres drybox or under an argon atmosphere using standard Schlenk techniques unless otherwise specified. Toluene and hexane were purified by passing through columns of activated alumina and activated Cu-0226 S copper catalyst (Engelhard), and CH_2Cl_2 was distilled under Ar from P_2O_5. Starting materials (Mn(CO)$_5$Me,[11] Re(CO)$_5$Me,[19] phosphite,[10] and H(Et$_2$O)$_2$BAr$_F$[5]) were prepared according to literature methods. The reagents used for this and for other procedures were purchased from Aldrich, Acros, or Strem Chemical Co. and used as received. ^{1}H, ^{31}P, ^{13}C, and ^{11}B NMR spectra were recorded on a Varian Unity 300 spectrometer with field strengths of 300, 121, 75, and 96 MHz, respectively. ^{1}H and ^{13}C chemical shifts were referenced to the residual solvent resonance relative to TMS; ^{31}P and ^{11}B chemical shifts were referenced to external 85% H_3PO_4 and BF_3/Et_2O, respectively. The BAr$_F$ peaks are not reported in the ^{13}C NMR data and are virtually identical with those previously reported, regardless of the cationic fragment.[20] Infrared spectra were recorded on a Nicolet Avator 360 FT-IR spectrometer. Elemental analyses were performed in house on a Perkin-Elmer Series II CHNS/O Model 2400 analyzer.

***cis*-Mn(L)(CO)$_4$(Me) (8).** A mixture of Mn(CO)$_5$Me (1.05 g, 5.00 mmol) and L (0.74 g, 2.10 mmol) in toluene (40 mL) was refluxed for ca. 16 h under an Ar atmosphere. All volatiles were removed under vacuum to give an off-white solid. The solid was purified in air by flash silica gel column chromatography, with hexane and CH_2Cl_2 as eluent to give the product (1.40 g, 85%) as a white solid. ^{1}H NMR (CD_2Cl_2): δ −0.38 (d, 3H, J = 8.6 Hz), 0.79 (s, 3H), 4.23 (d, 6H, J = 4.2 Hz). ^{13}C NMR (CD_2Cl_2): δ −20.0, 15.4, 76.2. Anal. Calcd for $C_{10}H_{12}O_7$-PMn: C, 36.36; H, 3.64. Found: C, 36.42; H, 3.84.

Reaction of 8 with [Ph$_3$C][BAr$_F$]. To a mixture of **8** (4 mg) and [Ph$_3$C][BAr$_F$] (24 mg) in a 5 mm NMR tube was added CD_2Cl_2 (0.5 mL) at room temperature to afford a yellow solution. NMR spectra were recorded. ^{1}H NMR (CD_2Cl_2): δ 0.81 (s, 1.5 H), 0.87 (s, 1.5 H), 4.27 (d, 3H), J = 4.4 Hz), 4.38 (d, 3H, J = 4.2 Hz), 7.57 (s, 4H), 7.73 (s, 8H). ^{31}P NMR (CD_2Cl_2): δ 150.0, 156.1.

[*cis*-Mn(L)(CO)$_4$(Et$_2$O)][BAr$_F$] (5b). To a mixture of **8** (33.0 mg, 0.10 mmol) and H(Et$_2$O)$_2$BAr$_F$ (101.2 mg, 0.10 mmol) was added Et_2O (6 mL) at room temperature. The solution was stirred at room temperature for 30 min, and then hexane (12 mL) was layered on top of Et_2O. The mixture was cooled to −30 °C for ca. 16 h to give **5b** (100.0 mg, 80%) as colorless crystals. ^{1}H NMR (CD_2Cl_2): δ 0.89 (s, 3H), 1.19 (t, 6H, J = 8.0 Hz), 3.52 (q, 4H, J = 8.0 Hz), 4.44 (d, 6H, J = 4.1 Hz), 7.58 (s, 4H), 7.73 (s, 8H). ^{13}C NMR (CD_2Cl_2): δ 13.1, 15.1, 77.0

(19) Beck, W.; Raab, K. *Inorg. Synth.* **1990**, *28*, 15.
(20) Butts, M. D.; Scott, B. L.; Kubas, G. J. *J. Am. Chem. Soc.* **1996**, *118*, 11831.

(OCH_2), 77.9 (d, J = 6.7 Hz). Anal. Calcd for $C_{45}H_{31}BF_{24}O_8$-PMn: C, 43.13; H, 2.48. Found: C, 43.17; H, 2.49.

[*cis*-Mn(L)(CO)$_4$(*cis*-cyclooctene)][BAr$_F$] (5c). To a solution of **8** (66.0 mg, 0.20 mmol) and *cis*-cyclooctene (cco, 0.20 mL, excess) in CH_2Cl_2 (3 mL) at −78 °C was added [Ph_3C]-[BAr_F] (221.2 mg, 0.20 mmol) in CH_2Cl_2 (4 mL). The mixture was stirred for 40 min at −78 °C and 1 h at room temperature to give a yellow suspension. The mixture was filtered through Celite and dried under vacuum to afford a yellow solid residue. The residue was crystallized from mixed CH_2Cl_2/toluene/hexane (8 mL/8 mL/4 mL) at −30 °C to give the product (0.120 g, 46%) as yellow crystals. ^{1}H NMR (CD_2Cl_2): δ 0.84 (s, 3H), 1.59 (m, 6H), 1.94 (m, 4H), 2.56 (m, 2H), 4.29 (d, 6H, J = 4.8 Hz), 4.94 (m, 2H), 7.57 (s, 4H), 7.72 (s, 8H). ^{13}C NMR (CD_2-Cl_2): δ 14.9, 26.0, 29.9, 31.3, 78.1 (d, J = 6.6 Hz), 101.8 (CH). Anal. Calcd for $C_{49}H_{35}BF_{24}O_7$PMn: C, 45.65; H, 2.72. Found: C, 46.07; H, 2.67.

***cis*-Re(L)(CO)$_4$Me (9).** A mixture of $Re(CO)_5Me$ (0.170 g, 0.50 mmol) and L (0.074 g, 0.50 mmol) in toluene (15 mL) was refluxed for 20 h under an Ar atmosphere to give a yellowish suspension. Volatiles were then removed, and the residue was purified by flash silica gel column chromatography, with CH_2-Cl_2/hexane (2/1) as eluent to give **9** (0.221 g, 96%) as a white solid. ^{1}H NMR ($CDCl_3$): δ −0.38 (d, 3H, J = 8.6 Hz), 0.83 (s, 3H), 4.24 (d, 6H, J = 4.6 Hz). ^{13}C NMR (CD_2Cl_2): δ −38.7 (t, J = 4.0 Hz), 15.9, 32.7, 75.8. Anal. Calcd for $C_{10}H_{12}O_7$PRe: C, 26.03; H, 2.60. Found: C, 26.20; H, 2.80.

[*cis*-Re(L)(CO)$_4$(CH$_2$Cl$_2$)][BAr$_F$] (6a). CH_2Cl_2 (6 mL) was added to a mixture of **9** (0.139 g, 0.30 mmol) and [Ph_3C][BAr_F] (0.354 g, 0.32 mmol) to give a yellowish solution. The mixture was stirred for 20 min at room temperature. Then $(Me_3Si)_2O$ (6 mL) was added. The resulting mixture was cooled to −30 °C to give **6a** (0.310 g, 74%) as light yellow brick-shaped crystals. ^{1}H NMR ($CDCl_3$): δ 0.79 (s, 3H), 4.29 (d, 6H, J = 4.6 Hz), 5.31 (s, 2H, CH_2Cl_2), 7.54 (s, 4H), 7.70 (s, 8H). ^{13}C NMR (CD_2Cl_2): δ 15.1, 77.4 (d, J = 6.2 Hz). Anal. Calcd for $C_{42}H_{23}$-$BCl_2F_{24}O_7$PRe: C, 36.15; H, 1.65. Found: C, 36.71; H, 1.81.

[*cis*-Re(L)(CO)$_4$(OEt$_2$)][BAr$_F$] (6b). Et_2O (3 mL) was added to **6a** (prepared in situ from **9** (0.037 g, 0.080 mmol) in CH_2Cl_2) to give a yellowish solution. Hexane was added, and the mixture was cooled to −30 °C to give **6b** (0.060 g, 54%) as colorless crystals. ^{1}H NMR (CD_2Cl_2): δ 0.88 (s, 3H), 1.24 (t, 6H, J = 7.0 Hz), 3.99 (4H, J = 7.0 Hz), 4.41 (d, 6H, J = 4.6 Hz), 7.57 (s, 4H), 7.72 (s, 8H). ^{13}C NMR (CD_2Cl_2): δ 13.7, 15.4, 77.4 (d, J = 5.9 Hz), 80.2. Anal. Calcd for $C_{45}H_{31}BF_{24}O_8$PRe: C, 39.04; H, 2.24. Found: C, 39.22; H, 2.11.

[*cis*-Re(L)(CO)$_4$(*cis*-cyclooctene)][BAr$_F$] (6c). *cis*-Cyclooctene (0.15 mL) was added to a solution of **6a** (prepared in situ from **9** (0.042 g, 0.91 mmol) in CH_2Cl_2 (3 mL) at room temperature to give a yellow solution. The solution was stirred for 30 min at room temperature. Hexane (10 mL) was then added, and the mixture was cooled to −30 °C to give **6c** (0.091 g, 66%) as yellow crystals. ^{1}H NMR (CD_2Cl_2): δ 0.82 (s, 3H), 1.57 (m, 6H), 1.90 (m, 2H), 2.14 (m, 2H), 2.71 (d, 2H, J = 13.1 Hz), 4.33 (d, 6H, J = 4.4 Hz), 5.15 (m, 2H), 7.58 (s, 4H), 7.74 (s, 8H). ^{13}C NMR (CD_2Cl_2): δ 15.3, 26.0, 30.7, 32.7, 77.7, 97.6. Anal. Calcd for $C_{49}H_{35}BF_{24}O_7$PRe: C, 41.44; H, 2.47. Found: C, 41.58; H, 2.50.

{**[*cis*-Re(L)(CO)$_4$]$_2$(μ-H)**}{**BAr$_F$**} **(10).** Et_3SiH (0.15 mL) was added to **6a** (0.200 g, 0.14 mmol) in CH_2Cl_2 (4 mL) at room temperature. The solution was then stirred for 30 min at room temperature. Hexane was added, and the mixture was cooled to −30 °C to give **10** (0.091 g, 36%**)** as colorless crystals. ^{1}H NMR (CD_2Cl_2): δ −18.23 (t, 1H, J = 12.2 Hz), 0.83 (s, 6H), 4.32 (d, 12H, J = 4.8 Hz), 7.58 (s, 4H), 7.74 (s, 8H). ^{13}C NMR (CD_2Cl_2): δ 15.4, 33.3, 77.1 (d, J = 6.0 Hz). Anal. Calcd for $C_{50}H_{31}BF_{24}O_{14}P_2$SiRe: C, 34.17; H, 1.76. Found: C, 34.44; H, 1.67.

In another NMR scale reaction, Et_3SiH (3 μL, ca. 2 equiv) was added to **6a** (0.0130 g) in CD_2Cl_2 (ca. 0.5 mL) in a 5 mm NMR tube at −78 °C. NMR spectra were recorded at temperatures from −80 °C to room temperature. The NMR spectra below −40 °C corresponded to that for the sum of the two reagents, indicating that no reaction occurred. At 0 °C, a new ^{1}H NMR peak at −10.68 ppm (br) as well as a new ^{31}P NMR signal at 102.5 ppm started to show up. These new NMR signals were presumably due to the η^2-H−$SiEt_3$ σ complex **6d**. As the temperature was raised to 25 °C, the intensity of the −10.68 ppm signal slowly decreased while the signal corresponding to the hydride complex **10** appeared. The σ-complex signal disappeared completely within 10 min at 25 °C. Volatiles of the reaction mixture were subjected to GC-MS detection, which showed Et_3SiCl and $(Et_3Si)_2O$ as two major components.

***fac*-Re(L)$_2$(CO)$_3$Me (11).** A mixture of $Re(CO)_5Me$ (0.628 g, 2.00 mmol) and L (0.592 g, 4.00 mmol) in toluene (12 mL) was refluxed for 20 h under an Ar atmosphere to give a yellowish suspension. Volatiles were then removed, and the residue was purified by flash silica gel column chromatography, with CH_2Cl_2 as eluent to give **11** (0.690 g, 59%) as a white solid. ^{1}H NMR (CD_2Cl_2): δ −0.62 (t, 6H, J = 9.0 Hz), 0.76 (s, 6H), 4.20 (t, 12H, J = 2.9 Hz). ^{13}C NMR (CD_2Cl_2): δ −38.2 (d, J = 11.1 Hz), 15.8, 32.7, 76.1 (d, J = 6.5 Hz). Anal. Calcd for $C_{14}H_{21}O_9P_2$Re: C, 28.91; H, 3.61. Found: C, 28.63; H, 3.74.

[*fac*-Re(L)$_2$(CO)$_3$(CH$_2$Cl$_2$)][BAr$_F$] (7a). A mixture of **9** (0.0581 g) and [Ph_3C][BAr_F] (0.1106 g) in CH_2Cl_2 (4 mL) was stirred at room temperature for 20 min. Hexane (15 mL) was then layered on top of the CH_2Cl_2 solution, and the mixture was cooled at −30 °C to give a yellowish oil. The oil was triturated with hexane to give **7a** (0.1001 g, 66%) as a yellowish solid. ^{1}H NMR (CD_2Cl_2): δ 0.85 (s, 6H), 4.34 (t, 12H, J = 1.3 Hz), 7.57 (s, 4H), 7.72 (s, 8H). ^{13}C NMR (CD_2Cl_2): δ 15.5, 77.0. Anal. Calcd for $C_{46}H_{32}BCl_2F_{24}O_9P_2$Re: C, 36.46; H, 2.11. Found: C, 36.72; H, 2.12.

[*fac*-Re(L)$_2$(CO)$_3$(OEt$_2$)][BAr$_F$] (7b). A mixture of **11** (0.044 g, 0.076 mmol) and $H(OEt_2)_2BAr_F$ (0.077 g, 0.076 mmol) was dissolved in mixed Et_2O (1.5 mL) and CH_2Cl_2 (1.5 mL) solvents to give a colorless solution. The solution was stirred at room temperature for 30 min. Volatiles were then removed, and the resulting residue was crystallized from Et_2O/hexane at room temperature to give **7b** (0.090 g, 79%) as brick-shaped colorless crystals. ^{1}H NMR (CD_2Cl_2): δ 0.83 (s, 6H), 1.16 (t, 6H, J = 7.0 Hz, OCH_2CH_3), 3.93 (q, 4H, J = 7.0 Hz, OCH_2CH_3), 4.33 (d, 12H, J = 1.7 Hz), 7.57 (s, 4H), 7.72 (s, 8H). ^{13}C NMR (CD_2Cl_2): δ 13.2, 15.5, 76.8, 78.4 (OCH_2CH_3). Anal. Calcd for $C_{49}H_{40}BF_{24}O_{10}P_2$Re: C, 39.12; H, 2.66. Found: C, 39.29; H, 2.83. Complex **7b** can also be prepared by addition of Et_2O to complex **7a** in CH_2Cl_2.

[*fac*-Re(L)$_2$(CO)$_3$(*cis*-cyclooctene)][BAr$_F$] (7c). *cis*-Cyclooctene (0.15 mL) was added to a solution of **7a** (prepared in situ from **11** (0.0555 g, 0.096 mmol)) in a mixture of PhCl (2 mL) and toluene (10 mL). CH_2Cl_2 (1.5 mL) was then added, followed by hexane. The solution was cooled to −30 °C to give **7c** (0.121 g, 82%) as light yellow crystals. ^{1}H NMR (CD_2Cl_2): δ 0.80 (s, 6H), 1.55 (m, 6H), 1.82 (m, 2H), 1.99 (m, 2H), 2.68 (dd, 2H, J = 13.5, 3.4 Hz), 4.30 (t, 12H, J = 1.4 Hz), 4.86 (t, 2H, J = 5.6 Hz), 7.58 (s, 4H), 7.74 (s, 8H). ^{13}C NMR (CD_2Cl_2): δ 15.4, 26.0, 30.1, 32.7, 77.0, 93.4. Anal. Calcd for $C_{53}H_{44}$-$BF_{24}O_9P_2$Re: C, 41.32; H, 2.86. Found: C, 40.98; H, 2.85.

[*fac*-Re(L)$_2$(CO)$_3$(η^2-H−SiEt$_3$)][BAr$_F$] (7d). Et_3SiH (0.15 mL) was added to complex **7a** (prepared in situ from complex **11** (0.136 g, 0.234 mmol)) in CH_2Cl_2 (5 mL) at room temperature to give a colorless solution. The solution was allowed to stand for 30 min at room temperature; hexane was then added. The mixture was cooled to −30 °C to give **7d** (0.250 g, 69%**)** as colorless crystals. ^{1}H NMR (CD_2Cl_2): δ −10.43 (t, 1H, J_{PH} = 12.7 Hz, J_{SiH} = 66 Hz), 0.80 (s, 6H), 1.06 (m, 15H), 4.29 (t, 12H, J = 1.5 Hz), 7.58 (s, 4H), 7.75 (s, 8H). ^{13}C NMR (CD_2-Cl_2): δ 6.6, 7.3, 15.4, 33.4, 76.8. Anal. Calcd for $C_{51}H_{46}$-$BF_{24}O_{10}P_2$SiRe: C, 39.61; H, 2.98. Found: C, 39.39; H, 2.97.

X-ray Structure Determination of 5c, 10, and 7b. Crystals of **5c**, **10**, and **7b** were mounted from a matrix of mineral oil under argon gas flow. The crystal was immediately

placed on a Bruker P4/CCD/PC diffractometer and cooled to 203 K using a Bruker LT-2 temperature device. The data were collected using a sealed, graphite-monochromated Mo Kα X-ray source. A hemisphere of data was collected using a combination of φ and ω scans, with 30 s frame exposures and 0.3° frame widths. Data collection and initial indexing and cell refinement was handled using SMART[21] software. Frame integrations and final cell parameter calculations were carried out using SAINT[22] software. The data were corrected for absorption using the SADABS[23] program. Decay of reflection intensity was not observed.

The structures were solved in space groups $P2_1/n$ (**5c**), $C2/c$ (**10**), and $P\bar{1}$ (**7b**) using direct methods and difference Fourier techniques. The initial solution revealed the majority of all non-hydrogen atom positions. The remaining atomic positions were determined from subsequent Fourier synthesis. Hydrogen atom positions were fixed (C−H = 0.93 Å for aromatic, 0.96 Å for methyl, and 0.97 Å for methylene). The hydrogen atoms were refined using the riding model, with isotropic temperature factors fixed to 1.5 (methyl) or 1.2 (all other) times the equivalent isotropic U value of the carbon atom they were bound to. For structure **5c**, due to disorder, several BAr_F fluorine and two cco methylene atoms were refined in two half-occupancy positions. The final refinement included anisotropic temperature factors on all non-hydrogen atoms and converged with final residuals of R1 = 0.0602 and wR2 = 0.1761. For structure **10**, the bridging hydride position was found on the difference map and refined with isotropic temperature factors set to 0.08 Å^2. The final refinement included anisotropic temperature factors on all non-hydrogen atoms and converged to R1($I > 2\sigma$(I)) = 0.0277 and wR2 = 0.0811. For structure **7b**, the final refinement[4] included anisotropic temperature factors on all non-hydrogen atoms and converged with final residuals of R1($I > 2\sigma(I)$) = 0.0644 and wR2 = 0.1152. For all complexes, structure solution, refinement, graphics, and creation of publication materials were performed using SHELXTL NT.[24] Additional details of the data collection and structure refinement are listed in Table 2.

Acknowledgment. This work was supported by the Department of Energy, Office of Basic Energy Sciences, Chemical Science Division. We thank Dr. John G. Watkin for many helpful discussions.

Supporting Information Available: X-ray crystallographic data for the structures of compounds **5c**, **7b**, and **10**. This material is available free of charge via the Internet at http://pubs.acs.org.

OM0004693

(21) SMART, version 4.210; Bruker Analytical X-ray Systems, Inc., 6300 Enterprise Lane, Madison, WI 53719, 1996.
(22) SAINT, version 4.05; Bruker Analytical X-ray Systems, Inc., Madison, WI 53719, 1996.
(23) Sheldrick, G. M. SADABS, first release; University of Göttingen, Göttingen, Germany.
(24) SHELXTL NT, version 5.10; Bruker Analytical X-ray Instruments, Inc., Madison, WI 53719, 1997.